FLOW OSCILLATION OVER AIRFOILS NEAR STALL

ICAS-94-4.5.2

Michael. B. Bragg, Associate Professor
Douglas C. Heinrich, Graduate Research Assistant
University of Illinois at Urbana-Champaign
Urbana, Illinois 61801
USA

K.B.M.Q. Zaman, Aerospace Engineer
NASA Lewis Research Center
Cleveland, Ohio 44135
USA

ABSTRACT

The flowfield about a LRN(1)-1007 airfoil was examined for Reynolds numbers from 0.3 to 1.2×10^6 at angles of attack from α = 0 to 28 degrees. Using a hot-wire sensor in the wake, a low-frequency flow oscillation was observed between α = 13.2 and 17 degrees at a Strouhal number near 0.02. Bluff body shedding was observed at higher α's with Strouhal numbers of 0.20. During the low-frequency oscillation the Strouhal number increased slightly with Reynolds number, but increased significantly with angle of attack. Using fluorescent surface oil flow visualization and laser sheet visualization of the off-body flow, the flowfield was examined more closely. The airfoil has a leading-edge laminar bubble followed by turbulent separation downstream near x/c=0.70 at angles of attack above 6 degrees. As the angle of attack for oscillation onset is approached, the bubble size grows rapidly and the turbulent separation point moves upstream. At α = 15 deg. the laser sheet flow visualization shows that the airfoil flowfield oscillates between an attached and separated state. It appears that the bubble grows, bursts and reforms at the measured oscillation frequency. The frequency compares roughly to shear layer flapping as observed by others in flows involving separation bubbles.

INTRODUCTION

It is well known that airfoils at angles of attack well beyond stall, and bluff bodies, experience flow oscillation at the nondimensional shedding frequency or Strouhal number S_t of approximately 0.20. Here, the Strouhal number, St = fcsinα/U, is based on airfoil projected height (csinα) and the free-stream velocity (U). However, many airfoils also exhibit a low-frequency flow oscillation at or near stall where S_t = 0.02. Jones[1] reported "violent fluctuations" of lift and drag of airfoils occurring around the angle of maximum lift. The oscillations were of very low frequency and could be estimated from Jones' data to correspond to S_t = 0.006. Jones also classified the stall of airfoils into three types: trailing-edge stall, thin airfoil stall and leading-edge stall. He observed that this low-frequency flow oscillation occurred for the first two stall types, but was absent for the third type. In addition, he noted that the large fluctuations occurred at maximum lift for the thin-airfoil-stall airfoils, but occurred a few degrees above maximum lift for trailing-edge-stall airfoils. Farren[2], using a fast response balance, observed a low-frequency oscillation on a R.A.F. 28x1.07 airfoil at α = 14 deg. and $R_e = 10^6$. The observed Strouhal number corresponded to $S_t \approx 0.019$.

In a study of acoustic excitation of the flow over a low-Reynolds number airfoil Zaman, Bar-Server and Mangalam[3] encountered a low-frequency flow oscillation. These tests were conducted on a LRN(1)-1007 airfoil at Reynolds numbers between 40,000 and 140,000, and the Strouhal number was 0.02. This oscillation occurred at an angle of attack of 15 degrees and could be suppressed by high frequency acoustic excitation of the flow.

A detailed study of the low-frequency flow oscillation on the LRN(1)-1007 airfoil was reported by Zaman, McKinzie and Rumsey[4]. They conducted an experimental and computational study of this phenomenon at low Reynolds number, $R_e < 300{,}000$. The oscillation was found to be hydrodynamic in nature and involved a quasi-periodic switching between stalled and unstalled conditions. The corresponding force oscillations were extremely large with ΔC_l of approximately 0.50. The Strouhal numbers observed were usually between 0.02 and 0.03. For $R_e < 10^5$, the oscillation did not occur naturally in the tunnel which had a free-stream turbulence level of 0.1%. A turbulence generating grid which raised the free-stream turbulence level to 0.4%, or high-frequency acoustic excitation, was required to "excite" the flow oscillation. This, coupled with other evidence, suggests that a transitional boundary layer at separation is required to

produce the phenomenon. The computational study, using a thin-layer Navier-Stokes code with the Baldwin-Lomax turbulence model, produced a flow oscillation at S_t = 0.03 only when transition was placed near the leading edge.

The bulk of the data in Ref. 4 were taken on a LRN(1)-1007 airfoil at low Reynolds number. It was not clear whether this low-frequency flow oscillation would persist at higher Reynolds number. Bragg, Heinrich and Khodadoust[5] extended the Reynolds number range to 1.4×10^6. The oscillation persisted up to this value and the Strouhal number was found to increase slightly with increasing Re. These data also suggested an increase in St with angle of attack, but a detailed study of this phenomenon was not conducted.

Recent experimental evidence indicates that the oscillation occurs on other airfoils at higher Reynolds numbers. Bragg and Khodadoust[6] observed a flow oscillation near stall with S_t = 0.018 on a NACA 0012 airfoil with simulated glaze ice. The airfoil was tested at $R_e = 1.5 \times 10^6$ and the flow oscillation was observed using hot-wire anemometry. Reda[7] observed a similar phenomenon when using liquid crystal flow visualization on a SAND 0018/50 airfoil at $R_e = 10^6$. He described the flow as "a quasiperiodic switching of the flow between separated and attached states over large portions of the airfoil lee surface". Using frame-by-frame analysis of the flow visualization, an oscillation frequency corresponding to a Strouhal number of 0.005 was estimated.

The low-frequency flow oscillation on airfoils near stall has been observed on several airfoils over a large range of Reynolds numbers. However, it has only received detailed study at low Reynolds numbers, and its exact origin has not to date been identified. The objective of this study was to identify the origin of the low-frequency oscillation. The LRN(1)-1007 airfoil was tested since it was known to readily produce this phenomenon. The previously identified, but not exploited, features[4,5] of dependence of the Strouhal number on Re and α were thoroughly documented using a hot-wire sensor in the wake. Flow visualization was used to observe the oscillating flowfield and document the steady flowfield leading up to the onset of the unsteady flow. A more complete set of these data are presented and discussed by Heinrich[8]. In this paper, the data are analyzed to provide a better understanding of the flowfield and the possible link between the observed flow oscillation and the leading-edge laminar separation bubble.

EXPERIMENTAL METHODS AND APPARATUS

Wind Tunnel and Model

The experiment was conducted in the University of Illinois subsonic wind tunnel. The tunnel is an open-circuit wind tunnel with a contraction ratio of 7.5:1,a 2.8 ft. x 4 ft. x 8 ft. test section and a maximum speed of approximately 160 mph. The tunnel uses honeycomb and 4 screens to achieve a turbulence intensity in the test section of under 0.1 %. Tunnel dynamic pressure was determined by a Δp measurement between the test section and settling chamber. A 0.1 psid transducer was used at low tunnel speeds and a 0.5 psid transducer at the higher speeds. The airfoil model was installed between two turntables located in the floor and the ceiling of the test section spanning the 2.8 ft height of the tunnel, Fig. 1.

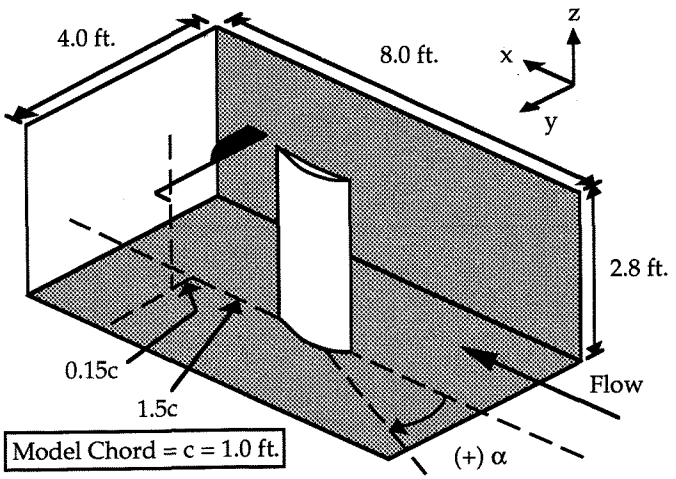

Figure 1. Airfoil model in the wind tunnel test section.

The airfoil used for this experiment was an LRN(1)-1007 section which has been described by Mangalam and Pfenninger[9]. The LRN(1)-1007 airfoil was designed for operation at low speeds and high altitudes. This combination results in low Reynolds number, thus the LRN designation. Earlier work by Zaman, McKinzie and Rumsey[4] showed that while other airfoils exhibit the low-frequency phenomenon, the LRN(1)-1007 produced it most readily; therefore, this airfoil was chosen for the present study. The solid aluminum model has a 1 ft. chord and 2.8 ft. span. The model contained no instrumentation and was painted flat black to facilitate the flow visualization.

Flow Visualization

Flow visualization was performed using a fluorescent oil technique. This technique uses oil on the surface to indicate flow direction and the relative surface shear levels. The oil used for this study was standard motor oil with a fluorescent dye added. The airfoil was illuminated using two ultra-violet fluorescent lamps, located on the top and bottom of the test

section. It should be noted that Plexiglas filters ultra-violet light; therefore, it was necessary to replace the Plexiglas side wall with glass.

The application of the oil was achieved by using a sponge and by dabbing the oil into place. This resulted in an uneven texture which facilitated the oil flowing process. Once the oil was applied, the tunnel was run at the desired conditions until a steady oil pattern was observed in the oil application. The oil flow was photographed using a standard 35mm camera after the pattern was established. In addition, the entire oil flow process was videotaped using a Sony Hi 8 mm camera. This helped resolve the flow direction and the rate at which the oil flowed, which was useful in interpreting the results.

The laser light sheet used in this experiment was produced by a 5 W Argon-Ion laser. The mirrors and glass rod were arranged such that the laser sheet was produced at the mid-span of the airfoil. The flow was seeded by atomizing a mixture of 50% water and 50% propylene glycol (PEG 400) by volume. The droplets were approximately 1 micron in diameter and introduced into the tunnel ahead of the turbulence screens. Then utilizing the Plexiglas turntable on the top of the tunnel, the results were recorded by the 30 frame per second video camera and by a 4.5 frame per second Canon SLR camera with an auto winder.

Hot-Wire

To identify the shedding frequency, f, a TSI IFA 100 anemometer with a T1.5 constant temperature hot-wire was used. The hot-wire was located one chord length downstream of the trailing edge and 0.15 chord above the mid-chord point as Zaman, McKinzie and Ramsey[4] had done and as shown in Fig. 1. A steel probe support with a symmetric airfoil crossection was introduced into the flow from the rear tunnel wall (the under surface of the airfoil) to hold the probe in the flow with a minimum of vibration. The natural frequency of the support was considerably above the flow frequencies of interest.

The output of the hot-wire anemometer was filtered at a high-pass frequency of 0.1 Hz, a low-pass frequency of 500 Hz, and was gained by 30 before being processed by the digital signal analyzer. The signal entering the signal analyzer was transformed using a discrete Fourier transform to values of spectral energy. Each transform used the Hanning weight function and was averaged eight times. A personal computer with an A/D board was used to record the tunnel speed from a wind tunnel Δp transducer, an absolute atmospheric pressure transducer and a thermocouple. The signal analyzer data were transferred to the computer using the IEEE board.

Data Reduction and Error Analysis

Flow visualization results were used to determine the chordwise location of laminar separation bubbles, boundary-layer transition and separation. This was done visually from the photographs using known model dimensions to scale the results. The accuracy of the chordwise locations reported are estimated to be within ± 2 percent chord.

The flow frequency in the model wake was determined from the hot-wire measurements and nondimensionalized to obtain the Strouhal number ($St = fc\sin\alpha/U$). Using the method of Coleman and Steele[10] the uncertainty in St can be estimated. For the purpose of determining the frequency, the spectrum analyzer was operated using a 10 Hz span which provided a 0.05 Hz resolution of the flow frequency. The angle of attack could be set to within 0.05 deg. and the tunnel Δp measured to within 0.14 percent of the transducer full-scale value. Using these values, the estimated uncertainty in the reported Strouhal number does not exceed 2 percent over the range of tunnel speeds and angles of attack where the wake frequency is clearly defined. However, at the angles of attack where the oscillation was weak, the flow frequency was not well defined and the error in selecting the frequency was much larger than the reported resolution. In these cases, the uncertainty in the Strouhal number could grow to 5 - 10 percent of the measured value.

RESULTS AND DISCUSSION

The LRN(1)-1007 airfoil was tested in the wind tunnel with the Reynolds number varied from approximately 0.3×10^6 to 1.25×10^6 at angles of attack from 0 to 28 degrees. Flow visualization studies were performed for angles of attack from 0 to 16 degrees at Re=0.8 million for the oil flow and 0.1 million for the laser sheet. The hot-wire measurements were concentrated in the angle of attack range from 13 to 17 degrees where the airfoil was near stall and the low-frequency oscillation was known to exist[4,5]. First the airfoil flowfield from $\alpha = 0$ to 12 deg will be discussed. It is important to understand the development of the flowfield when attempting to interpret the more complex unsteady flow at the higher angles of attack. Using the flow visualization, results of airfoil analysis codes, etc. the flow over the airfoil is described. Next, the unsteady results, primarily from the wake hot-wire results, supplemented by the laser-sheet flow visualization, are presented. The emphasis in this section is the dependence of the low-frequency oscillation on the model angle of attack and Reynolds number and how this information can be used to help understand the phenomena.

Airfoil Flowfield For $0 \le \alpha \le 12$ deg.

The LRN airfoil was designed[9] for high-lift and low drag at a Reynolds numbers of 50,000 to 150,000. At low angles of attack, the airfoil has a shallow favorable

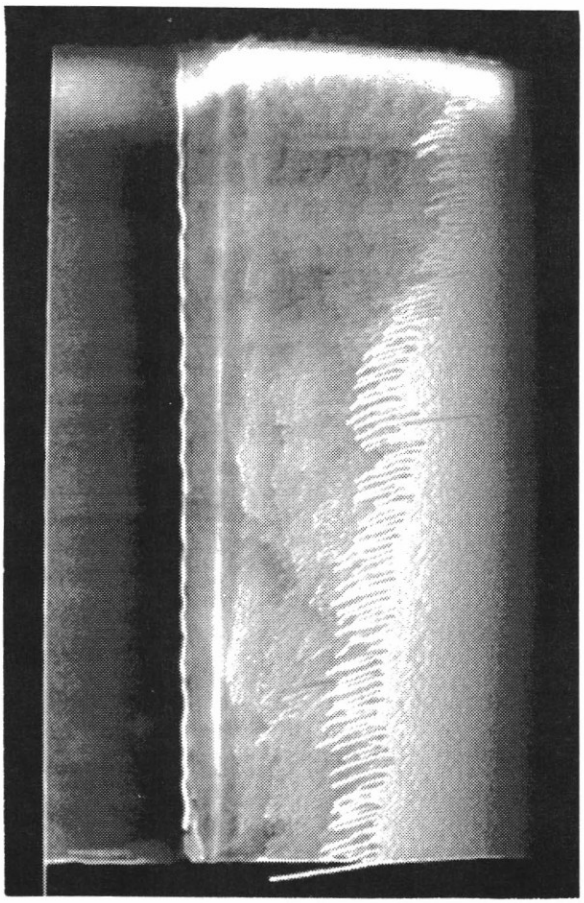

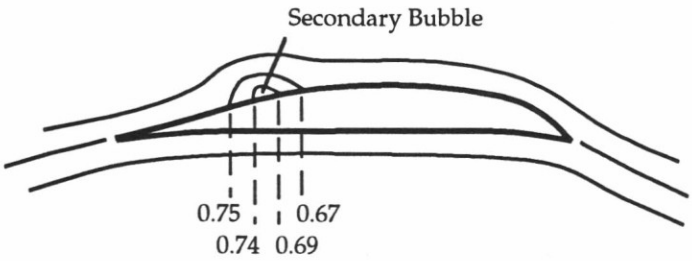

Fig. 2. Surface oil flow visualization and sketch of the flowfield at α=2 deg. and Re=0.8x10^6 (flow right to left).

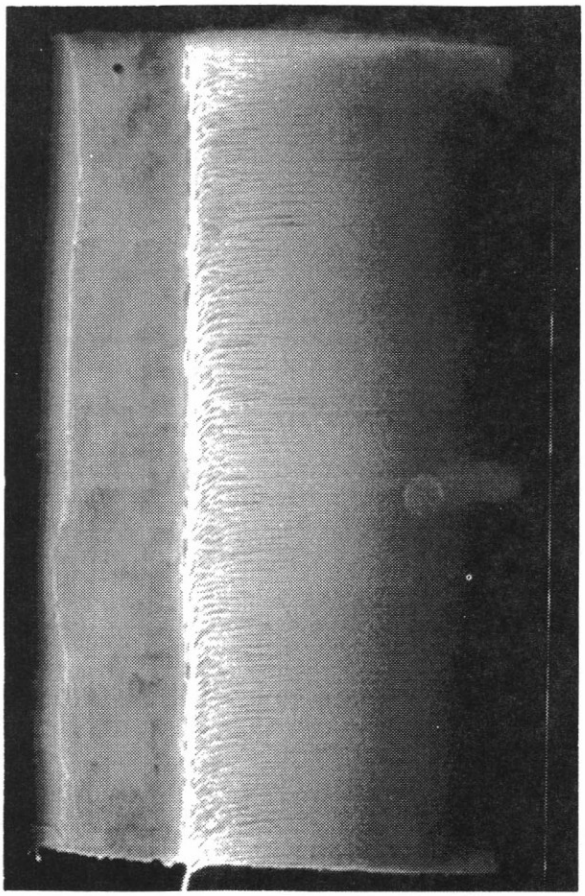

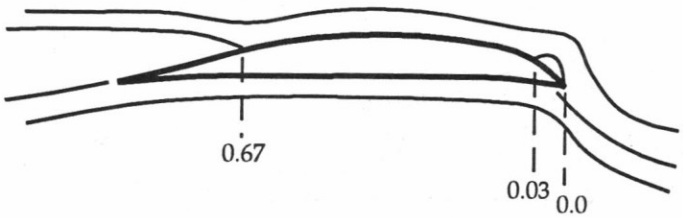

Fig. 3. Surface oil flow visualization and sketch of the flowfield at α=10 deg. and Re=0.8x10^6 (flow right to left).

pressure gradient on the upper surface from just aft of the leading edge back to approximately 75 percent chord. At this point, a fairly severe adverse gradient exists to 78 percent chord, followed by a more moderate recovery back to the trailing-edge. The results of this design, tested here at a significantly higher Reynolds number than the design value, can be clearly seen in the surface oil flow visualization. In fact, the flowfield can be divided into three regimes based on the angle of attack.

The first flow regime exists between approximately 0 and 4 degrees angle of attack. In this case the flow on the upper surface is laminar back to the start of the adverse pressure gradient where transition occurs and the pressure is recovered back to the trailing edge by the turbulent boundary layer. Transition takes place in a large laminar separation bubble. This is easily seen in the flow visualization photo, Fig. 2, taken on the upper surface at Re=0.8x10^6 and α=2 deg. A sketch of this flowfield, also shown in Fig. 2, was composed from information taken from the still photo and the video. Remember that oil pools on the surface at regions where the shear changes sign, i.e. where the flow separates from the surface. Here two lines are seen on the model in the area where a laminar bubble would be expected. Similar to the computational results of Davis and Carter[11], this airfoil experiences a laminar bubble with a secondary separation bubble. The laminar boundary

layer separates as indicated by the first line (note flow in Fig. 2 is right to left) at x/c=0.67 and reattaches at x/c=0.75, just downstream of the second oil line. This reattachment location is indicated by a faint line ahead of which the oil has been scrubbed upstream due to a large negative surface shear force. The oil that is scrubbed upstream forms the second distinct oil line at x/c=0.74. This is the location of the separation of the reverse flow which forms the secondary bubble, rotating in the opposite direction under the main or primary bubble. The secondary bubble reattaches at x/c=0.69 which is difficult to see in the still photos, but more easily distinguished in the video. The flow aft of x/c=0.75 is a turbulent boundary layer which, with its high shear, causes oil to flow downstream on the surface forming a bead of oil at the trailing edge.

The second flow regime covers the approximate angle of attack range from 6 to 12 degrees. Here, due to the changing pressure distribution, the transition location moves upstream to near the leading edge. The boundary layer is turbulent as it reaches the severe adverse gradient on the aft part of the airfoil and separates. For example, Fig. 3 shows that at α=10 deg. the laminar boundary layer separates from the leading edge, the separated shear layer becomes turbulent and reattaches at x/c=0.03, and the turbulent boundary-layer separates at x/c=0.67. This is similar to the behavior of the high-lift, low Re, laminar flow airfoil tested by Bragg and Gregorek[12]. This airfoil boundary layer separated at the start of the upper surface pressure recovery region when the boundary layer transitioned early due to surface roughness near the leading edge.

In Fig. 4, the behavior of the upper surface boundary layer as deduced from the flow visualization is shown for α's to 14 degrees. In the 6 to 12 deg. range the bubble grows slowly reaching only x/c=0.03 by α=12 deg. No evidence of a secondary bubble has been seen in this range of angles of attack. The trailing-edge separation, however, moves forward relatively quickly with increasing α reaching x/c=0.67 at α=12 deg. Note that the flowfield changes little between 10 and 12 degrees angle of attack. Above 12 degrees the flowfield begins to change rapidly with angle of attack as stall is approached and the unsteady flow begins.

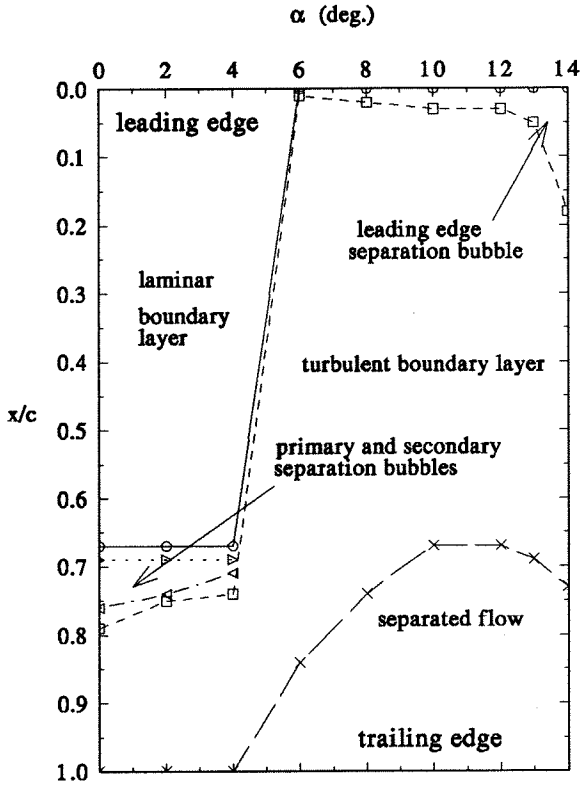

Fig. 4. Airfoil upper surface boundary-layer state for α = 0 to 14 deg. and Re = 0.8x10^6.

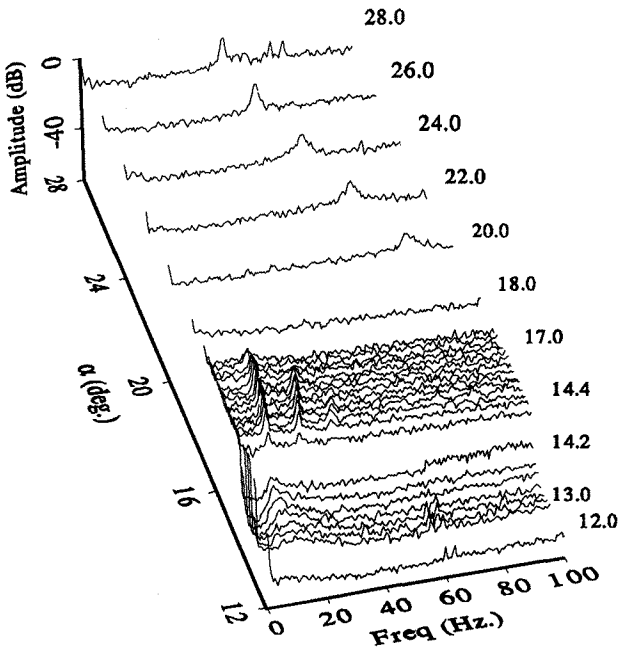

Fig. 5. Spectral energy in the wake for α = 12 to 28 deg. and Re = 0.8x10^6.

Airfoil Unsteady Flowfield For α > 13 deg.

The low-frequency flow oscillation was first observed by Zaman, Mckinzie and Rumsey[4], and later confirmed by Bragg, Heinrich and Khodadoust[5] on the LRN(1)-1007 airfoil to exist in the approximate α range from 13 to 17 degrees. Figure 5 shows the spectral energy in the wake at Re=0.8x10^6 for angles of attack from 12 to 28 degrees. At α=13.2 deg., the first evidence of the low-frequency oscillation can be seen at a frequency of approximately 11 Hz. This peak in energy is clearly visible by 14 deg and at a frequency only slightly higher. Between 14.6 and 16.4 degrees angle of attack the first harmonic can be seen as well.

The fundamental is the low-frequency oscillation which, if converted to a Strouhal number using the airfoil height, csinα, as the characteristic length, results in a value around 0.02. This is only 10 percent of the usual bluff body shedding value. In fact, bluff body shedding can be seen at α's of 20 deg. and above at frequencies around 50 to 75 Hz. These frequency values decrease with increasing α to maintain a constant St around 0.20 since the characteristic length, the airfoil height, increases with α.

Since the best definition of the low-frequency oscillation appears to be at approximately 15 degrees angle of attack, Fig. 6 depicts the amplitude of the wake spectral energy versus frequency and tunnel velocity. The fundamental, first and to some extent the second harmonic can be identified. The frequencies of the observed spectral peaks increase linearly with increasing velocity. The velocity range covered in Fig. 6 corresponds to a Re range from $0.3x10^6$ to $1.2x10^6$. Over this range, the amplitude of the low-frequency oscillation is fairly constant with Re. The linearity of these results with velocity strongly suggests a flow phenomena, and in fact Zaman, Mckinzie and Rumsey[4] carefully explored alternate explanations and deduced that it was indeed fluid dynamic in nature. The question remains, what is the source of this flow oscillation? The answer to this question remains incomplete, however, the following observations can be made to gain further insight.

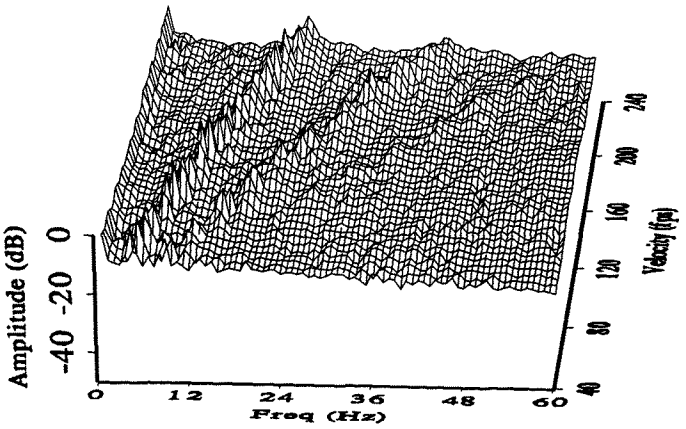

Fig. 6. Spectral energy as a function of frequency and velocity at α = 15 deg.

Consider first the upper surface flowfield information presented in Fig. 4. Above 12 degrees angle of attack the leading-edge separation bubble grows rapidly as the angle of attack is increased reaching x/c=0.18 at α=14 deg. Remember that this information was obtained primarily from surface oil flow which is a steady state technique. At α=14 deg., the flow appeared to be well behaved and the bubble reattachment location and boundary-layer separation location well defined. Surface flow visualization at α=15 was very different from 14 deg.; with what appears to be a large, but ill defined, bubble to about x/c=0.50, followed by a very low shear region to x/c=0.63 and an apparent separated region aft of x/c=0.63. This information was not included on Fig. 4 due to the uncertainty in defining these regions. At α=16 deg., the low shear region grows to cover a majority of the upper surface. The rapidly growing, but well defined leading-edge bubble at α=14 deg, followed by the large separated regions with ill defined boundaries at α=15 deg., indicates large regions of unsteady separation developing on the airfoil upper surface between these two angles of attack.

The relationship between the low-frequency flow oscillation and unsteady flow separation is well supported by other evidence. Zaman, Mckinzie and Rumsey[4] measured large force oscillations on the LRN(1)-1007 airfoil while observing this low-frequency oscillation which suggests large-scale flow unsteadiness. During this test, although no measurements were made, large model vibrations were observed. Smoke-wire flow visualization and computational results[4] have shown large vortical structures being shed during the low-frequency oscillation. Reda[7] observed the low-frequency oscillation on an airfoil using surface visualization with liquid crystals. He reports a "quasi-periodic switching of the flow between separated and attached states over large portions of the airfoil lee surface".

The laser sheet flow visualization reveals the unsteady separation phenomena. Figure 7 shows a sequence of photos taken with the laser sheet with the flow seeded with 1 micron particles and the tunnel at a speed of 8 mph or $Re=0.075x10^6$. The flow is from left to right and the airfoil upper surface is seen as the thin white line formed by the intersection of the laser sheet and the model. The camera location is above and behind the airfoil section illuminated by the laser sheet. At this low velocity the oscillation was measured at approximately 1 Hz. The photos were taken at approximately 0.0225 seconds between frames. Although seen more clearly in the video, the leading-edge separation bubble grows and then bursts causing the flow on the upper surface to separate to the trailing edge. A vortex appears to form on the upper surface and is convected downstream and off the airfoil. As the vortex leaves the airfoil, the flow reattaches. In Fig. 7 the flow is reattaching in the top photo, is reattached in the second, the bubble has grown significantly by the third, and in the bottom photo the airfoil is completely separated. This separation and reattachment occurs at the same frequency as that measured in the wake by the hot-wire sensor.

From the surface flow visualization, this unsteady separation appears to start in earnest between 14 and 15 degrees angle of attack. The exact angle can be

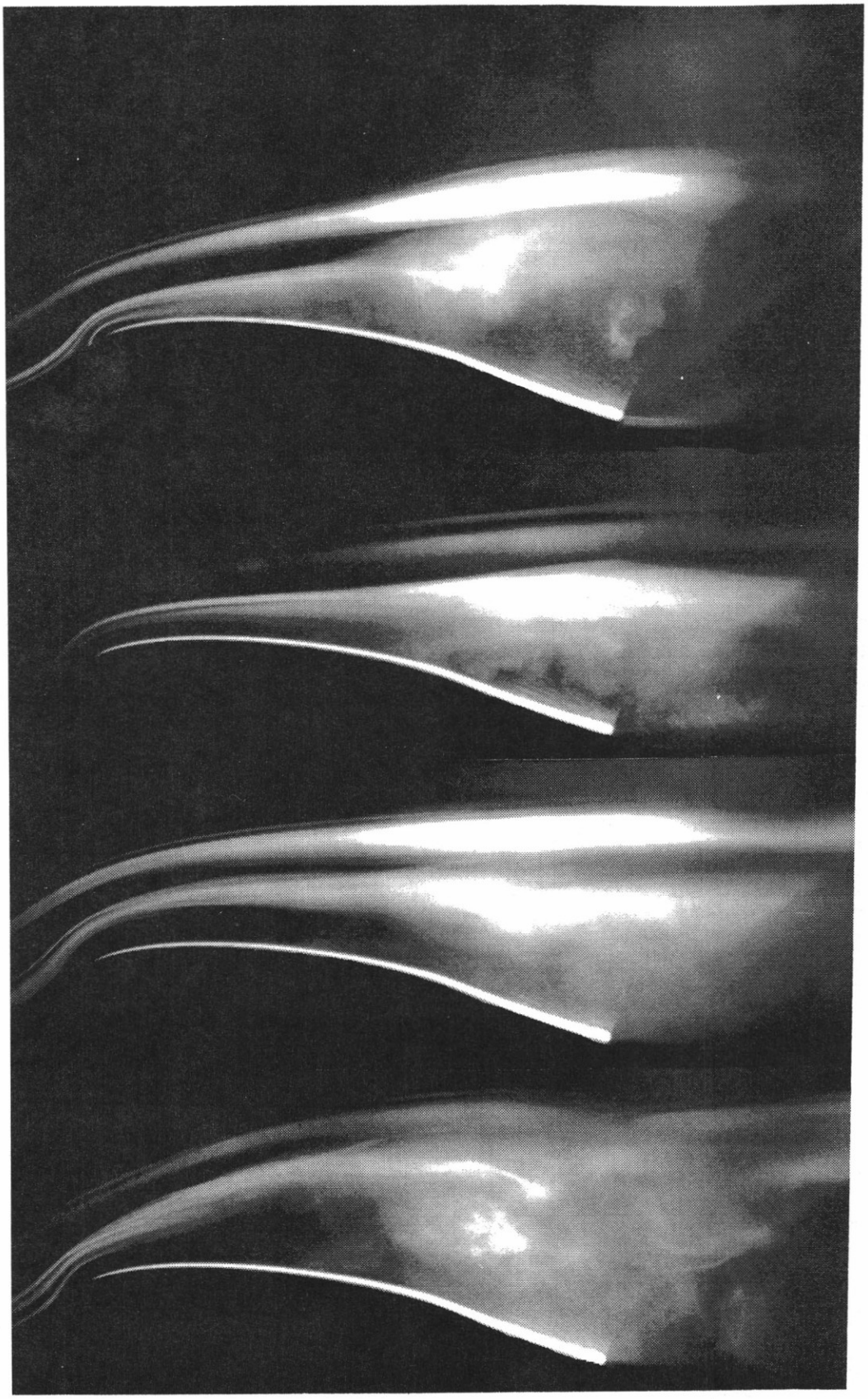

Fig. 7 Laser sheet flow visualization on the upper surface at Re = 0.075×10^6 and α = 15 deg. with the sequence of photos from the top to the bottom, 0.0225 secs apart (flow from left to right).

better determined from the hot-wire data. From Fig. 5 the overall energy in the frequency spectra increases significantly over the entire frequency range when the angle of attack is increased from 14.2 to 14.4 degrees. This would seem to indicate that the unsteady separation phenomenon begins, or at least gains significant strength, between α = 14.2 and 14.4 degrees.

It is apparent that the low-frequency oscillation is associated with the unsteady behavior of a leading-edge separation bubble. In Gaster's classic paper[13] on laminar separation bubbles, he notes a low-frequency oscillation in the bubble in addition to higher frequency unsteadiness. Gaster speculates that this corresponds to a vertical motion of the shear layer. This vertical motion of a shear layer is usually referred to as shear layer flapping. Heinrich[8] took Gaster's observed frequency and used the generating airfoil height as the characteristic length, to obtain a Strouhal number similar to the 0.02 value measured in this study.

More recent studies of the unsteadiness of separated shear layers have provided additional information on the flapping phenomenon. The flapping occurs in separated shear layer flows generated from many geometries, for example: backward-facing step flows[14], a surface mounted fence[15], a pipe inlet[16] and a blunt flat plate flow[17]. These examples represent both laminar and turbulent boundary-layer separation, but the laminar shear layers quickly transition. Cherry et. al.[17] comment that low-frequency shear layer flapping is a feature of a fully turbulent separation. This may explain why in Ref. 4, at low Reynolds numbers, the low-frequency oscillation was observed only when artificial boundary-layer tripping or increased free-stream turbulence was added to the flow.

In a separated shear layer the flow phenomenon of vortex roll-up and pairing is well known. The nondimensional frequency of this disturbance is about 0.20 if the shear layer height and mean velocity are used as the characteristic length and velocity scale, respectively. Mabey[18] correlated unsteady pressure measurements in separated flows and found the same frequency, although he nondimensionalized it using free-stream velocity and bubble length to get a value in the range of 0.6 to 0.9. For most flows, the majority of the unsteady energy is in these higher frequencies due to the shear layer vortical structures[14,17], with significantly less energy in the lower shear layer flapping range.

Shear layer flapping corresponds to large changes in the shear layer reattachment zone. Driver et. al.[14] describes the flapping as the result of a large vortex in the shear layer which escapes and goes downstream without any of its mass being entrained in the bubble. This causes the bubble to collapse and the curvature of the shear layer near reattachment to increase. The pressure gradient increases and more mass is captured in the bubble to fill it up and the cycle continues. Cherry et. al.[17] note that the flapping and vortex shedding is pseudoperiodic, i.e. not at equal intervals in time. This can be seen in their data as no distinct frequency for vortex shedding is seen in the spectral analysis of the pressure or velocity data. Rather, the flapping energy is spread over a wide frequency band. They also observed that near separation, before the shear layer vortical structures have reached significant strength, more than half of the energy in the unsteady pressure was at nondimensional frequencies below 20 percent of the shear layer vortical frequency. This compares to the frequency range seen in these experiments where the low-frequency oscillation is approximately 10 percent of the bluff body shedding value.

The low-frequency oscillation seen in the wake of this airfoil appears to correspond to the frequency range of the shear layer flapping observed by others[13-18]. This airfoil was shown to have a laminar leading-edge separation bubble with turbulent reattachment in the lower angle of attack range of the observed low-frequency oscillation. Shear layer flapping causes an oscillation in the bubble reattachment location which might be triggering the low-frequency flow oscillation. The present flow is somewhat different in that the low-frequency oscillation is much more periodic and energetic than that seen by others on different geometries. This is most likely due to the high angle of attack which generates very adverse pressure gradients in the bubble reattachment region. It may also relate to an interaction with the trailing-edge separation. This might explain in part why airfoils with leading-edge stall, sudden flow separation from the leading edge with no reattachment, do not exhibit the low-frequency oscillation[1].

The hot-wire measurements showed a strong dependence of the Strouhal number on the airfoil angle of attack and Reynolds number . Figure 8 shows Strouhal number versus Reynolds number for angles of attack from 14.4 to 16.6 degrees. This is the angle range where the oscillation frequency is clearly distinguishable. St increases slightly with Re, but increases significantly with angle of attack. Figure 9 shows these trends more clearly. The Strouhal number versus angle of attack data are at $Re=0.8x10^6$ and include angles of attack above and below that shown in Fig. 8. The Strouhal number is fairly constant from α = 13.6 to 14.4 deg., increases linearly with α from 14.4 to 16.6 deg. and is constant from α = 16.6 to 17 deg. During the linear region St increases from 0.02 to 0.029 with a slope of 0.00458/deg. The change in St with Reynolds number, $\Delta St/\Delta Re$, is more modest and is a function of angle of attack as shown in Fig. 9. The change in St with Re is less at the higher angles of

attack. The value of $\Delta St/\Delta Re$ is almost 0.004 per million Re at α = 14 deg., 0.0015 at α = 16 deg. and has an average slope over this range of 0.00246 per million Re. The source of these changes in St are not known. However, note that the St versus α data in Fig. 9 begin its linear growth at the angle of attack where the large flow separations are thought to begin. If the proper scaling is average bubble length as used by Mabey[18], then the increasing St as defined here, which results from increasing oscillation frequency, would suggest a decreasing average bubble length. Unfortunately, average bubble length could not be determined from the oil flow in this angle of attack range and no other measurements are available. These changes in St with Re and α provide clues to the flowfield which will be explored in future studies.

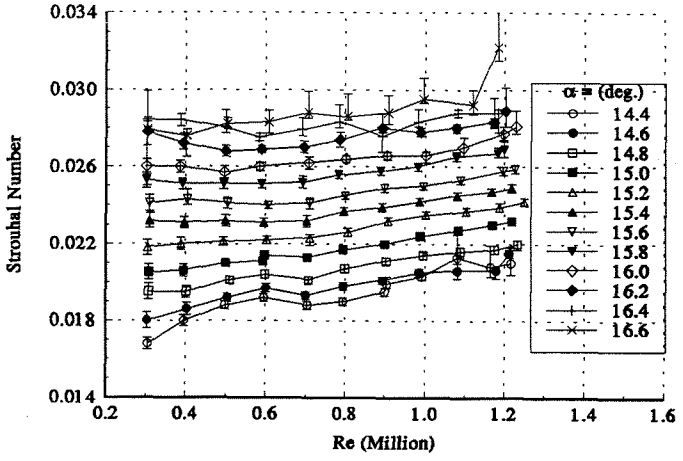

Fig. 8. Strouhal number of the low-frequency oscillation as a function of α and Re.

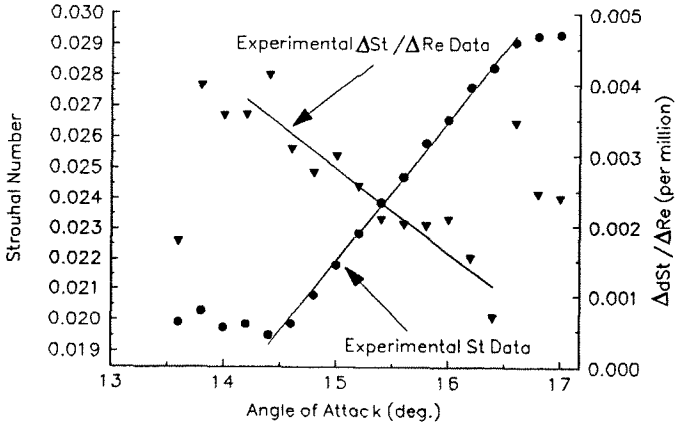

Fig. 9. Effect of α and Re on the Strouhal number: St versus α at Re=0.8×10^6.

SUMMARY and CONCLUSIONS

The flowfield about a LRN(1)-1007 airfoil was studied at Reynolds numbers from 0.3 to 1.2×10^6. Surface oil flow visualization showed a midchord laminar separation bubble at low angles of attack. In the angle of attack range from 6 to 12 deg., the flow on the upper surface transitioned in a leading-edge bubble, and the turbulent boundary layer separated at approximately x/c=0.70 at the start the pressure recovery region. Between α = 13.2 and 17.0 deg., the airfoil experienced a low-frequency flow oscillation with St = 0.02 to 0.03. Bluff body shedding near St = 0.20 was observed at higher angles of attack. The St of the low-frequency oscillation increased significantly with angle of attack in the range α = 14.4 to 16.6 deg. A small increase in St with Re was also observed.

The low-frequency oscillation appears to be associated with the flapping of the laminar separation bubble shear layer. The nondimensional frequencies in the present case compare well to corresponding values of low-frequency unsteadiness in separated and reattached flows observed by others. In previous studies the energy at the flapping frequencies were observed to be small and the motion quasiperiodic. However, these corresponding flows did not experience the bursting of the bubble. In the present airfoil case, the flow oscillation becomes more periodic and energetic, probably due to, or as a result of, the shear layer flapping inducing the airfoil separation and the resulting vortex shedding. The growth of the bubble, vortex shedding, and a subsequent repetition of the process was observed in the flow visualization.

The low-frequency flow oscillation has been studied only at fairly low Reynolds numbers. However, the flapping of bound shear layers in separating and reattaching flows has been observed in turbulent backward facing step flows. In fact, Cherry et. al.[17] state that shear layer flapping is a phenomenon associated with turbulent shear layers. This would suggest that the low-frequency flow oscillation over airfoils near stall may occur at higher Reynolds numbers as well. During this study, no significant reduction was seen in the energy in the low-frequency oscillation as the Reynolds number was increased from 0.3 to over 1.2×10^6.

ACKNOWLEDGMENT

The authors wish to thank Dr. A. Khodadoust for his assistance in acquiring and analyzing these data. Mr. T. Balow's assistance in preparing this paper is gratefully acknowledged. The authors at the University of Illinois were supported in part by grant NAG 3-1374 from NASA Lewis Research Center.

REFERENCES

1. Jones, B. M., "An Experimental Study of The Stalling of Wings", *Aeronautical Research Committee Reports and Memoranda* No. 1588, 1933.
2. Farren, W. S., "The Reaction on a Wing Whose Angle of Incidence is Changing Rapidly. Wind Tunnel Experiments With a Short Period Recording Balance", *Aeronautical Research Committee Reports and Memoranda* No. 1648, 1935.
3. Zaman, K.B.M.Q., Bar-Sever, A. and Mangalam, S. M., "Effect of Acoustic Excitation on the Flow Over a Low-Re Airfoil", *Journal of Fluid Mechanics*, Vol. 182, 1987, pp. 127-148.
4. Zaman. K.B.M.Q., McKinzie, D. J. and Rumsey, C. L., "A Natural Low-Frequency Oscillation of the Flow Over an Airfoil Near Stalling Conditions", *Journal of Fluid Mechanics*, Vol. 202, 1989, pp. 403-422.
5. Bragg, M. B., Heinrich, D. C. and Khodadoust, A., "Low-Frequency Oscillation over Airfoils near Stall", *AIAA Journal*, Vol. 31, No. 7, July 1993, pp. 1341-1343.
6. Bragg, M. B. and Khodadoust, A., "Experimental Measurements in a Large Separation Bubble Due to a Simulated Glaze Ice Accretion", AIAA Paper No. 88-0116, Jan. 1988.
7. Reda, D. C. "Observations of Dynamic Stall Phenomena Using Liquid Crystal Coatings", *AIAA Journal*, Vol. 29, No. 2, 1991, pp. 308-310.
8. Heinrich, D. C., "An Experimental Study of a Low Frequency Flow Oscillation over a Low Reynolds Number Airfoil Near Stall", M.S. Thesis, University of Illinois at Urbana-Champaign, 1994.
9. Mangalam, S. M., and Pfenninger, W., "Wind-Tunnel Tests on a High Performance Low-Reynolds Number Airfoil," AIAA Paper 84-0628, 1984.
10. Coleman, H. W. and Steele, W. G., *Experimentation and Uncertainty Analysis For Engineers*, John Wiley and Sons, New York, 1989.
11. Davis, R. L., and Carter, J. E., "Analysis of Airfoil Transitional Separation Bubbles," NASA Contractor Report 3791, 1984.
12. Bragg, M. B. and Gregorek, G. M., "Experimental Airfoil Performance with Vortex Generators", *Journal of Aircraft*, Vol. 24, No. 4, 1987, pp. 305-309.
13. Gaster, M., "The Structure and Behavior of Separation Bubbles," Aeronautical Research Committee Reports and Memoranda No. 3595, His Majesty's Stationery Office, London, March, 1967.
14. Driver, D. M., Seegmiller, H. L., and Marvin, J., "Unsteady Behavior of a Reattaching Shear Layer," AIAA Paper 83-1712, 1983.
15. Fricke, F. R., "Pressure Fluctuations in Separated Flow", *J. Sound Vib*, vol. 17, 1971, pp. 113-123.
16. McGuinness, M. D., "Flow With a Separation Bubble: Steady and Unsteady Aspects", Ph.D. thesis, University of Cambridge, 1978.
17. Cherry, N. J., Hillier, R. and Latour, M.E.M.P., "Unsteady Measurements in a Separated and Reattaching Flow", *Journal of Fluid Mechanics*, Vol. 144, 1984, pp. 13-46.
18. Mabey, D. G., "Analysis and Correlation of Data on Pressure Fluctuations in Separated Flow", *Journal of Aircraft*, Vol. 9, No. 9, 1972, pp. 642-645.